J. Fluid Mech. (2022), *vol*. 952, A30, doi:10.1017/jfm.2022.911

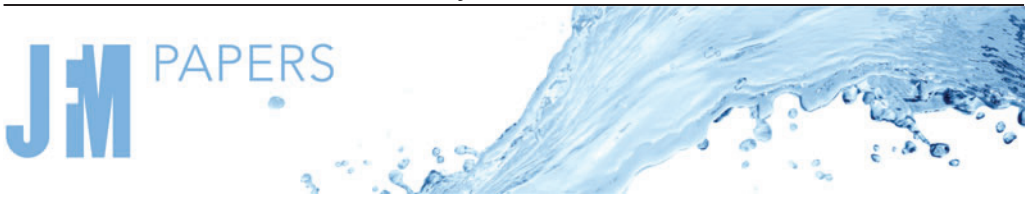

Free surface in two-dimensional potential flow: singularities, invariants and virtual fluid

A.I. Dyachenko[1,2,3], **S.A. Dyachenko**[4,†] **and V.E. Zakharov**[5]

[1]Landau Institute for Theoretical Physics, Chernogolovka 142432, Russia

[2]Skolkovo Institute of Science and Technology, Moscow, Russia

[3]National Research University Higher School of Economics, Myasnitskaya 20, Moscow 101000, Russia

[4]Department of Mathematics, University at Buffalo, SUNY Buffalo, NY 14260, USA

[5]Department of Mathematics, University of Arizona, Tucson, AZ 85721, USA

(Received 24 March 2022; revised 14 October 2022; accepted 23 October 2022)

We study a two-dimensional (2-D) potential flow of an ideal fluid with a free surface with decaying conditions at infinity. By using the conformal variables approach, we study a particular solution of the Euler equations having a pair of square-root branch points in the conformal plane, and find that the analytic continuation of the fluid complex potential and conformal map define a flow in the entire complex plane, excluding a vertical cut between the branch points. The expanded domain is called the 'virtual' fluid, and it contains a vortex sheet whose dynamics is equivalent to the equations of motion posed at the free surface. The equations of fluid motion are analytically continued to both sides of the vertical branch cut (the vortex sheet), and additional time invariants associated with the topology of the conformal plane and Kelvin's theorem for a virtual fluid are explored. We called them 'winding' and virtual circulation. This result can be generalized to a system of many cuts connecting many branch points, resulting in a pair of invariants for each pair of branch points. We develop an asymptotic theory that shows how a solution originating from a single vertical cut forms a singularity at the free surface in infinite time, the rate of singularity approach is double exponential and supersedes the previous result of the short branch cut theory with finite time singularity formation. The present work offers a new look at fluid dynamics with a free surface by unifying the problem of motion of vortex sheets, and the problem of 2-D water waves. A particularly interesting question that arises in this context is whether instabilities of the virtual vortex sheet are related to breaking of steep ocean waves when gravity effects are included.

Key words: contour dynamics, surface gravity waves

† Email address for correspondence: sergeydy@buffalo.edu

1. Introduction

Motion of an ideal fluid with a free surface is one of the oldest problems in applied mathematics, and the emergence of complex analysis can be attributed to the study of potential flows in two dimensions. A fluid flow that is coupled to the motion of a free boundary, as in the motion of waves at the surface of an ocean, becomes particularly rich and complex. Many classical problems in nonlinear science are tied to the dynamics of the ocean surface: the nonlinear Schröedinger equation and the Korteweg–de-Vries equation both can be derived as an approximation to water wave motion under distinct assumptions. Yet both models share a particularly striking property: integrability. Integrable systems are quite rare, and one of their special features is a dynamics that is uniquely determined by a set of integrals of motion and phases, also referred to as action and angle variables see e.g. Kolmogorov (1954). The state of an integrable system at a given time can be determined by means of the inverse scattering technique; see the works on integrable systems (Gardner *et al.* 1967; Zakharov & Faddeev 1971; Shabat & Zakharov 1972; Ablowitz *et al.* 1974; Zakharov & Shabat 1974, 1979).

At present, many nonlinear systems have been discovered, yet integrability of the full water wave system remains elusive. The search for integrability in water waves is a long standing problem, and it was proven that, if it indeed exists, it is of a special kind. Dyachenko, Lvov & Zakharov (1995) applies the Zakharov–Schulman technique to water waves and shows that the fluid dynamics is not integrable with a time-invariant spectrum. Nevertheless, new non-trivial integrals of motion have been discovered Tanveer 1993; Dyachenko *et al.* 2019, 2021; Lushnikov & Zakharov 2021) that suggest the presence of a hidden structure, suggesting integrability in a broader sense. The new integrals of motion are related to contour integrals in the analytic continuation of the fluid domain, the 'virtual fluid' (also sometimes referred to as phantom and/or unphysical), which is an abstraction defining a fluid flow in a maximally extended domain where the analytic functions defining the flow reach their natural boundaries of analyticity. In the preceding work (Dyachenko *et al.* 2019) the authors found that, if a singularity of the complex velocity in the virtual fluid is a pole, then its residue is a time invariant. Nevertheless, the appearance of isolated singularities in a generic flow is observed under very special circumstances (Galin 1945; Polubarinova-Kochina 1945; Zakharov & Dyachenko 1996). Even then, isolated singularities alone are incompatible with a fluid flow with a free surface; see the work Lushnikov & Zakharov (2021). Exact solutions originally found by Dirichlet and described in Longuet-Higgins (1972) are second-order curves and also contain square-root branch points. A notable exception is a classical work of Crapper (1957), who discovered the travelling wave on a free surface subject to forces of surface tension; the Crapper waves are one of the few exact solutions and their singularities are isolated poles; the work of Crowdy (2000) discusses the mathematical framework to construct flows with surface tension and rational solutions in particular. The recent work by Dyachenko & Mikyoung Hur (2019) and the following theoretical proof by Mikyoung Hur & Wheeler (2020) show that Crapper waves also occur in the vanishing gravity limit for waves over a shear current.

The importance of square-root branch points for potential fluid flow has been first discovered in the work of Tanveer (1993). In the work of Baker & Xie (2011), the authors concluded that a square-root branch point approaches the fluid region when a breaking gravity wave becomes overhanging. Formation of a square-root singularity and whitecapping was also conjectured in Dyachenko & Newell (2016). The work of Castro *et al.* (2013) is a study of the formation of a multivalued surface through the 'splash'

mechanism: a scenario in which a free surface becomes self-intersecting; the authors show that splash singularity may appear in a finite time while originating from a perfectly smooth initial datum. The origin of the appearance of branch points is the complex Hopf equation (Kuznetsov, Spector & Zakharov 1993; Karabut & Zhuravleva 2014; Karabut, Zhuravleva & Zubarev 2020) that governs fluid motion in some approximation. Many non-trivial flows are described by square-root branch points; see for example the works by Dyachenko *et al.* (1996), Dyachenko, Zakharov & Kuznetsov (1996), Zakharov (2020) and Liu & Pego (2021) for the study of a free surface with decaying boundary conditions, and the recent work of Dyachenko *et al.* (2021) for the periodic case. To further the case, a periodic wave that is travelling on a free surface, also known as the Stokes wave, has square-root branch points as found in the work of Grant (1973) and a numerical study of its singularities in Dyachenko, Lushnikov & Korotkevich (2014, 2016) by means of a rational approximation (Alpert, Greengard & Hagström 2000), and the singularity of the limiting Stokes wave is conjectured to be the result of coalescence of multiple square-root branch points; see the work Lushnikov (2016).

Two-dimensional (2-D) fluid flows can be studied using the conformal variables approach, which was first introduced in the 19th century. The pioneering work of Stokes (1880) on travelling periodic waves discusses conformal mapping in the context of 120° at the crest; see also a recent review paper of Haziot *et al.* (2022) and references therein. The problem of finding standing waves is more mysterious, due to their complicated temporal dynamics. A recent work by Wilkening (2021) discusses a technique for construction of travelling–standing waves that bridge the gap between travelling and standing waves. The first application of conformal mapping to time-dependent flows can be traced to the work of Ovsyannikov (1973), that followed a result of Zakharov (1968) who discovered that the canonical Hamiltonian variables for fluid flow consist of the free surface and the velocity potential on it.

The conformal mapping technique is not always the most convenient way to study water waves numerically, and we will refer the reader to the work of Wilkening & Vasan (2015) for other highly efficient methods for 2-D fluid dynamics. The recent works by Arsénio, Dormy & Lacave (2020) and Ambrose *et al.* (2022) discuss novel methods for simulating the Euler equation in two dimensions, which generalize to 3-D water waves. The conformal mapping technique is discussed in the works of Tanveer (1991, 1993), Dyachenko *et al.* (1996) and Dyachenko (2001) and has been successfully applied numerically by many authors, see e.g. the works of Zakharov, Dyachenko & Vasilyev (2002) and Dyachenko & Newell (2016).

In the present work, we develop an exact theory of a potential 2-D flow in the Euler equations with a free surface. The theory describes a particular solution that carries a pair of square-root branch points in the analytic continuation of the complex velocity and the conformal map (see figure 1), and offers a pair of newly discovered integrals of motion, the 'winding' and 'circulation' of a virtual fluid. Asymptotic theory is developed that shows the double-exponential approach of a square-root branch point to the fluid domain that suggests the formation of a singularity in infinite time, which is distinct from the short branch-cut theory developed in preceding works.

2. The square-root branch cut

The nonlinear equations for the dynamics of the free surface of a 2-D fluid, written in conformal variables, have been known since the work of Ovsyannikov (1973) and

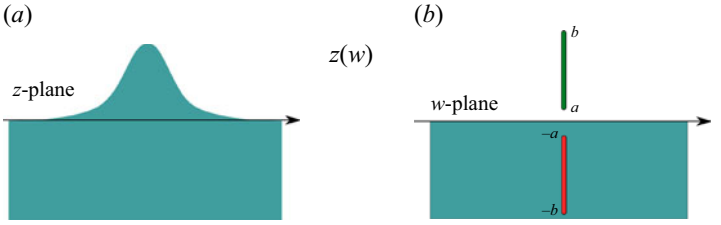

Figure 1. Schematics of conformal map z. The fluid region (green) is mapped to the lower complex plane $\mathrm{Im}\, w < 0$, the branch cut of R, V is marked in blue. The branch cuts for complex conjugate functions are marked red.

Tanveer (1991). We consider the form of these equations given in the work of Dyachenko (2001)

$$\left.\begin{aligned} \dot{R} &= \mathrm{i}\left(UR' - U'R\right) \\ \dot{V} &= \mathrm{i}\left(UV' - B'R\right) \end{aligned}\right\}. \tag{2.1}$$

The functions $R(w,t)$, $V(w,t)$, $U(w,t)$ and $B(w,t)$ are analytic with respect to complex variable $w = u + iv \in \mathbb{C}^-$ (the lower half-plane). Here, $U(w,t)$ and $B(w,t)$ are analytically continued from the real line, where they are given by the relations

$$U(u,t) = \hat{P}^-[\bar{V}(u,t)R(u,t) + V(u,t)\bar{R}(u,t)], \quad B(u,t) = \hat{P}^-[V(u,t)\bar{V}(u,t)]. \tag{2.2a,b}$$

where bar denotes complex conjugation.

Here, $\hat{P}^-$ is the projection operator from the real axis to the lower half-plane. Given on the real axis

$$\hat{P}^- = \frac{1}{2}(1 + i\hat{H}), \quad \hat{H}\text{- is the Hilbert transform: } \hat{H}f = p.v.\frac{1}{\pi}\int_{-\infty}^{\infty}\frac{f(u',t)du'}{u'-u}. \tag{2.3}$$

Let

$$R(w,t) = 1 + \rho(w,t), \quad \text{where } \rho(w\to\infty)\to 0. \tag{2.4}$$

The four analytic functions have square-root branch points at $w = \mathrm{i}a(t)$ and $w = \mathrm{i}b(t)$, and thus can be expressed by means of the Cauchy integral formula with the clockwise contour orientation

$$\rho(w,t) = \frac{1}{2\pi\mathrm{i}}\oint_{[\mathrm{i}a,\mathrm{i}b]}\frac{\rho(s,t)\,\mathrm{d}s}{s-w} = \frac{\mathrm{i}}{2\pi}\lim_{\varepsilon\to 0^+}\int_{\mathrm{i}a}^{\mathrm{i}b}\frac{[\rho(s+\varepsilon)-\rho(s-\varepsilon)]\,\mathrm{d}s}{s-w}, \tag{2.5}$$

and we denote $\rho(s\pm\varepsilon)\to\rho^{\pm}(s)$ as $\varepsilon\to 0^+$. Let $\tau = -\mathrm{i}s \in [a,b]$, then we rewrite the formula as follows:

$$\rho(w,t) = \frac{1}{2\pi}\int_a^b\frac{\left[\rho^+(\mathrm{i}\tau)-\rho^-(\mathrm{i}\tau)\right]\mathrm{d}\tau}{-\mathrm{i}\tau + w}, \tag{2.6}$$

and define jumps on the cut for ρ and V

$$r(\tau) = \frac{\rho^+(\mathrm{i}\tau)-\rho^-(\mathrm{i}\tau)}{2\mathrm{i}} \quad \text{and} \quad v(\tau) = \frac{V^+(\mathrm{i}\tau)-V^-(\mathrm{i}\tau)}{2\mathrm{i}}, \tag{2.7a,b}$$

and note that $r(a) = r(b) = 0$ and $v(a) = v(b) = 0$. The associated analytic functions are then given by

$$R(w,t) = 1 - \frac{1}{\pi}\int_a^b \frac{r(\tau)\,\mathrm{d}\tau}{\tau + \mathrm{i}w} \quad \text{and} \quad V(w,t) = -\frac{1}{\pi}\int_a^b \frac{v(\tau)\,\mathrm{d}\tau}{\tau + \mathrm{i}w}. \tag{2.8a,b}$$

We also introduce the two additional functions from the following relations to introduce U and B:

$$\bar{R}V + R\bar{V} = V + \bar{V} + \frac{1}{\pi^2}\iint \frac{\left[\bar{r}(\tau')v(\tau) + r(\tau)\bar{v}(\tau')\right]\mathrm{d}\tau\,\mathrm{d}\tau'}{(\tau + \mathrm{i}w)(\tau' - \mathrm{i}w)}, \tag{2.9}$$

$$\bar{V}V = \frac{1}{\pi^2}\iint \frac{v(\tau)\bar{v}(\tau')\,\mathrm{d}\tau\,\mathrm{d}\tau'}{(\tau + \mathrm{i}w)(\tau' - \mathrm{i}w)} \tag{2.10}$$

We refer the reader to the derivation in Appendix A of the following formulas:

$$U(w) = -\frac{1}{\pi}\int \frac{u(\tau)\,\mathrm{d}\tau}{\tau + \mathrm{i}w} \quad \text{and} \quad B(w) = -\frac{1}{\pi}\int \frac{b(\tau)\,\mathrm{d}\tau}{\tau + \mathrm{i}w}, \tag{2.11a,b}$$

where $u(\tau) = v(\tau)\bar{R}(\mathrm{i}\tau) + r(\tau)\bar{V}(\mathrm{i}\tau)$ and $b(\tau) = v(\tau)\bar{V}(\mathrm{i}\tau)$ for $\tau \in [a, b]$.

2.1. *Boundary values of analytic function at the cut*

Before proceeding, one must be able to evaluate the complex analytic function by its associated jump on the cut. Given $\varepsilon > 0$, one finds that

$$R(\mathrm{i}\tau \pm \varepsilon) = 1 - \frac{1}{\pi}\int_a^b \frac{r(\tau')\,\mathrm{d}\tau'}{\tau' - \tau \pm \mathrm{i}\varepsilon} \quad \text{and} \quad V(\mathrm{i}\tau \pm \varepsilon) = -\frac{1}{\pi}\int_a^b \frac{v(\tau')\,\mathrm{d}\tau'}{\tau' - \tau \pm \mathrm{i}\varepsilon}, \tag{2.12a,b}$$

and we may apply the Sokhotskii–Plemelj theorem to obtain

$$R^{\pm}(\mathrm{i}\tau) = \lim_{\varepsilon\to 0^+} R(\mathrm{i}\tau \pm \varepsilon) = 1 - (\hat{H} \mp \mathrm{i})r(\tau), \tag{2.13}$$

$$V^{\pm}(\mathrm{i}\tau) = \lim_{\varepsilon\to 0^+} V(\mathrm{i}\tau \pm \varepsilon) = -(\hat{H} \mp \mathrm{i})v(\tau), \tag{2.14}$$

where we have defined the integral operator $\hat{H}$ as follows:

$$\hat{H}f(\tau) = \frac{1}{\pi}v.p.\int_a^b \frac{f(\tau')\,\mathrm{d}\tau'}{\tau' - \tau}. \tag{2.15}$$

Similar relations hold for the functions U and B.

2.2. *Equations of motion on the cut*

The equations of motion in w-plane have been derived previously, and are given by

$$\partial_t R = \mathrm{i}\left(UR_w - U_w R\right), \tag{2.16}$$

$$\partial_t V = \mathrm{i}\left(UV_w - B_w R\right), \tag{2.17}$$

and can be written in terms of the jumps of the associated functions as follows:

$$\left.\begin{aligned} r_t + u\hat{H}r' + r'\hat{H}u + u'(1-\hat{H}r) - r\hat{H}u' = 0 \\ v_t + u\hat{H}v' + v'\hat{H}u + b'(1-\hat{H}r) - r\hat{H}b' = 0 \end{aligned}\right\}. \tag{2.18}$$

Given a square-root branch point in $z(w) = \sqrt{w - \mathrm{i}a}$, the function $R = 1/z_u \sim \sqrt{w - \mathrm{i}a}$ vanishes at the branch points. Similarly, it is trivial to show that $R(w, t)$ has zeros at the branch points $\mathrm{i}a$ and $\mathrm{i}b$

$$R(\mathrm{i}a) = R(\mathrm{i}b) = 0 \quad \text{and} \quad R(w \to -\mathrm{i}\infty) \to 1, \tag{2.19a,b}$$

as the solution evolves the branch points do not vanish, but move in the complex plane, see Dyachenko *et al.* (2021).

One can use the shifted Chebyshev basis to efficiently represent the complex analytic functions with a pair of square-root singularities. We introduce the centre of the cut, $c(t) = (a(t) + b(t))/2$, and its half-length, $l(t) = (b(t) - a(t))/2$, and use $f_n(w, t)$ as a basis for expansion of the analytic functions $R(w, t)$ and $V(w, t)$. It is convenient to work with the variable $\xi(w, t) = (c + \mathrm{i}w)/l$, then

$$f_n(\xi) = \left[\xi - \sqrt{\xi^2 - 1}\right]^n = (-1)^n \left[T_n(-\xi) + U_{n-1}(-\xi)\sqrt{\xi^2 - 1}\right], \tag{2.20}$$

where $T_n(\xi)$ and $U_{n-1}(\xi)$ for $n = 1, 2, \ldots$ are the Chebyshev polynomials of the first and the second kinds, respectively. Note that $w \in [\mathrm{i}a, \mathrm{i}b]$ is mapped to $\xi \in [-1, 1]$ for convenience.

2.3. *Expansion of $R(w, t)$ and $V(w, t)$*

The complex velocity, V, and R may be expanded in the form

$$V(\xi, t) = \sum_{k=1}^{\infty} v_k(t) f_k(\xi) \quad \text{and} \quad R(\xi, t) = 1 + \sum_{k=1}^{\infty} r_k(t) f_k(\xi). \tag{2.21a,b}$$

In order to satisfy the conditions (2.19*a*,*b*) we have two additional constraints on the coefficients of R that must be satisfied for any $t > 0$

$$\sum_{k=1}^{\infty} r_k(t) = \sum_{k=1}^{\infty} (-1)^k r_k(t) = -1. \tag{2.22}$$

It is convenient to rewrite the series defined in relations (2.21*a*,*b*) and (2.20) using the following substitution:

$$\xi = \cos\chi \quad \text{or, equivalently} \quad w = \mathrm{i}c - \mathrm{i}l\cos\chi, \quad \chi = \eta + \mathrm{i}\zeta, \tag{2.23}$$

where $\chi \in [-\pi, \pi]$ is mapped to $\xi \in [-1, 1]$. Moreover, the relation (2.23) defines a conformal mapping for complex w, such that $\chi(w \in \mathbb{C}) \to \mathbb{C}^-$ (see also the illustration in figure 2), and the free surface (blue–white boundary) is located at

$$\chi(u) = \mathrm{i}\ln\left[\xi - \sqrt{\xi^2 - 1}\right], \quad \text{where } \xi = \frac{c + \mathrm{i}u}{l}. \tag{2.24}$$

Note that the square root in (2.24) is so that $\sqrt{a^2\,\mathrm{e}^{\mathrm{i}\phi}} = |a|\exp(\mathrm{i}(\phi/2))$.

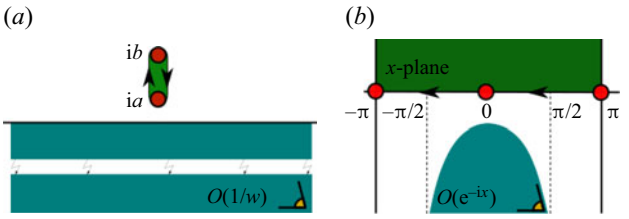

Figure 2. Schematics of χ-map. A periodic strip $-\pi \le \mathrm{Re}\,\chi < \pi$ and $\mathrm{Im}\,\chi < 0$ (right) is mapped to $w \in \mathbb{C} \cap [ia, ib]$ (left), and the $\mathrm{Im}\,\chi > 0$ (right) is mapped to the second sheet of the w-plane. (*a*) The blue region is mapped to the fluid domain (the real fluid), and the upper half-plane marked white excluding the cut is the virtual fluid in the first sheet outside the cut. The red circles mark the locations of the branch points, and arrows indicate the positive orientation for a Cauchy-type integral (2.5). An observer marked with an eye that is located far away from the cut (large distance from real line is illustrated by the lightning symbols) sees the dominant term of a far field $1/w$ whose coefficient is a motion integral defined in (2.34*a*,*b*). The green domain observed on the left is the virtual fluid of the second Riemann sheet which is seen through the cut. (*b*) After the conformal map (2.23) the image of a periodic contour around the cut is mapped to the interval $[-\pi, \pi]$, and the Chebyshev function basis (2.20) becomes the standard Fourier basis (2.25). The image of the real fluid is located in the lower complex plane enclosed within vertical asymptotes $\chi = \pm\pi/2$ (dashed lines), and the virtual fluid from the first sheet is mapped to the white region in the lower half-plane. The second Riemann sheet is unfolded into the upper half-plane of the χ-plane. The singularities in the upper half-plane of χ are located in the second Riemann sheet of w-plane, and can be studied numerically and theoretically.

The components of the Chebyshev series

$$f_n(\xi) = \left[\xi - \sqrt{\xi^2 - 1}\right]^n = \exp(-\mathrm{i}n\chi), \tag{2.25}$$

become the standard Fourier series in χ variable in negative Fourier harmonics. Note that all functions R, V, U, B and their complex conjugates in the w-plane can be expanded in the series (2.25) with $n \ge 0$

$$V(\chi, t) = \sum_{k=1}^{\infty} v_k(t) \exp(-\mathrm{i}k\chi) \quad \text{and} \quad R(\chi, t) = 1 + \sum_{k=1}^{\infty} r_k(t) \exp(-\mathrm{i}k\chi). \tag{2.26a,b}$$

In order to determine the functions U and B we will first evaluate the auxiliary functions $u(\tau)$ and $b(\tau)$ at the cut. Then, we will use the Sokhotskii–Plemelj theorem to find the values of U and B at the cut, $\chi = \eta + \mathrm{i}0 \in [-\pi, \pi]$. The values of R and V at the reflection of the contour around the cut in the lower half-plane of w can be determined in the χ-plane. The reflection of the cut is located on the negative imaginary axis at $\chi = 0 + \mathrm{i}\zeta_{cc}(\tau)$ given by the relation

$$\left.\begin{aligned} \cos \mathrm{i}\zeta_{cc} &= \frac{c+\tau}{l}, \\ \cos \mathrm{i}\zeta_{cc} &= 2 + 2\frac{a}{l} - \xi = 2 + 2\frac{a}{l} - \cos\eta, \end{aligned}\right\} \tag{2.27}$$

where $\tau \in [a, b]$ (see also the formula (2.11*a*,*b*)). Note that the right-hand side of the formula is strictly greater than 1, and the values of ζ_{cc} are purely real and negative, given our choice of the mapping $\chi(w)$. Solving for ζ_{cc}, we find

$$\zeta_{cc}(\xi) = -\ln\left[y + \sqrt{y^2 - 1}\right] = -\,\mathrm{acosh}\, y, \tag{2.28}$$

where $y = 2 + 2(a/l) - \xi$. The functions $\bar{R}$ and $\bar{V}$ can then be found on the reflection of the cut $w \in [-\mathrm{i}a, -\mathrm{i}b]$ (or equivalently $\chi \in \mathrm{i}\zeta_{cc}$) by evaluating the formulas

$$\left.\begin{aligned} \bar{R} &= 1 - \pi \sum_{k=1} k_n \left(\sqrt{y^2-1} - y\right)^k = 1 - \pi \sum_{n=1} r_k (-1)^k \exp(k\zeta_{cc}), \\ \bar{V} &= -\pi \sum_{k=1} v_k \left(\sqrt{y^2-1} - y\right)^k = -\pi \sum_{k=1} v_k (-1)^k \exp(k\zeta_{cc}). \end{aligned}\right\} \tag{2.29}$$

We may now form the functions $u = V\bar{R} + \bar{V}R$ and $b = V\bar{V}$ and find the boundary values of analytic functions U and B as follows:

$$\left.\begin{aligned} U(\eta) &= \frac{1}{2\pi\mathrm{i}} \int_{-\pi}^{\pi} \frac{u(-\eta') - u(\eta')}{2} \cot \frac{\eta' - \eta}{2} \mathrm{d}\eta', \\ B(\eta) &= \frac{1}{2\pi\mathrm{i}} \int_{-\pi}^{\pi} \frac{b(-\eta') - b(\eta')}{2} \cot \frac{\eta' - \eta}{2} \mathrm{d}\eta', \end{aligned}\right\} \tag{2.30}$$

which can be efficiently computed by means of the fast Fourier transform.

2.4. *Equations in χ-plane and integrals of motion*

By making additional transformation (2.23) the equations of motion become particularly simple, and are given by the following relations:

$$-l \sin\eta R_t - \left(\dot{c} + \dot{l}\cos\eta\right) R_\eta = \mathrm{i}\left(UR_\eta - U_\eta R\right), \tag{2.31}$$

$$-l \sin\eta V_t - \left(\dot{c} + \dot{l}\cos\eta\right) V_\eta = \mathrm{i}\left(UV_\eta - B_\eta R\right). \tag{2.32}$$

These equations have two integrals of motion which are equivalent to the ones found in Tanveer (1993). Indeed, one can integrate equations (2.31) using expansion (2.26*a*,*b*). As a result, the following expressions are valid:

$$\begin{cases} r_1 l(t) = -2Q = const \\ v_1 l(t) = -2\Gamma = const \end{cases} \quad \Rightarrow \quad \mathrm{e}^{-\mathrm{i}\chi} = -\frac{l(t)}{2w} \quad \text{as } w \to \infty, \tag{2.33}$$

or

$$R(w) = 1 + \frac{Q}{w} + O\left(\frac{1}{w^2}\right), \quad V(w) = \frac{\Gamma}{w} + O\left(\frac{1}{w^2}\right) \quad |w| \to \infty, \tag{2.34a,b}$$

where Q and Γ are called 'winding' and virtual 'circulation'. Conservation of circulation can be viewed as Kelvin's theorem for a virtual fluid, and winding is related to the topology of the conformal plane.

2.5. *Formation of singularity in infinite time*

We shall consider the lowest-order expansion so that the initial datum satisfies the constraints (2.19*a*,*b*) and still results in a non-trivial fluid flow. The functions R and V

at time $t = 0$ are given by

$$V(\xi) = lf_1(\xi) = \mathrm{i}[w - \mathrm{i}c - \sqrt{(w - \mathrm{i}c)^2 + l^2}] \tag{2.35}$$

$$R(\xi) = 1 - f_2(\xi) = [1 + \frac{1}{l^2}(w - \mathrm{i}c - \sqrt{(w - \mathrm{i}c)^2 + l^2})^2]. \tag{2.36}$$

It is assumed that, at least for some time, these functions are given by convergent series of the form (2.21*a*,*b*), or equivalently the Fourier series (2.26*a*,*b*). This is a crucial assumption that is only based on the results of numerical simulations of the short branch cut (Dyachenko *et al.* 2021), and preceding theoretical work (see Tanveer 1993; Dyachenko *et al.* 2019). Approximately speaking, this assumption will hold when the only zeros of R in the first Riemann sheet are located at the branch points. Naturally, one must ensure that the initial data (2.35)–(2.36) have no additional zeros in the first sheet.

In order to establish the motion of the branch points we seek the complex conjugated functions given by

$$\tilde{V} = -\mathrm{i}[w + \mathrm{i}c - \sqrt{(w + \mathrm{i}c)^2 + l^2}], \tag{2.37}$$

$$\tilde{R} = \left[1 + \frac{1}{l^2}(w + \mathrm{i}c - \sqrt{(w + \mathrm{i}c)^2 + l^2})^2\right]. \tag{2.38}$$

Then, we must calculate all four functions V, $\tilde{V}$, R and $\tilde{R}$ on the imaginary axis by replacing $w \to \mathrm{i}v$. We introduce

$$S = \sqrt{(v - a)(v - b)} = \sqrt{l^2 - (v - c)^2}, \tag{2.39}$$

$$F = \sqrt{(v + a)(v + b)} = \sqrt{(v + c)^2 - l^2}. \tag{2.40}$$

Now

$$V = -v + c - \mathrm{i}S, \tag{2.41}$$

$$\tilde{V} = v + c - F, \tag{2.42}$$

and we may write

$$R = 1 - \frac{(v - c + \mathrm{i}S)^2}{l^2} = \frac{2}{l^2}[S^2 - \mathrm{i}(v - c)S], \tag{2.43}$$

$$\tilde{R} = 1 - \frac{(v + c - F)^2}{l^2} = \frac{2}{l^2}F\,(v + c - F)\,. \tag{2.44}$$

Then we introduce

$$Q = R\tilde{V} + \tilde{R}V, \tag{2.45}$$

to end up with transport velocity U

$$U = P^{-}Q. \tag{2.46}$$

Notice that the singularities of Q in the upper half-plane are the ones coming from the function S. We can replace $Q \to Q_{ess}$ where Q_{ess} only includes the terms proportional to S.

A simple calculation reveals the following expression:

$$Q_{ess} = \frac{2\mathrm{i}}{l^2}\left[2lFS - \left(c^2 + ab + 2cv\right)S\right]. \tag{2.47}$$

Then

$$U = \left(1 - \mathrm{i}\hat{H}\right)Q_{ess}, \tag{2.48}$$

where $\hat{H}$ is the Hilbert transform. To calculate the 'Hilbert' transform one should remember that, after projecting to the lower half-plane, Q_{ess} must be replaced by its analytic continuation to the upper half-plane. This is done by restoring the regular part by the corresponding singular part as in formula (2.20). It amounts to writing

$$\mathrm{i}S \to \mathrm{i}S - (v - c), \tag{2.49}$$

$$\mathrm{i}vS \to \mathrm{i}vS - v(v - c) + \tfrac{1}{2}l^2. \tag{2.50}$$

Collecting all terms together we find following expression for transport velocity U:

$$U = Q_{ess} + \frac{2}{l^2}\left[2cv^2 + abv - c\left(c^2 + \frac{l^2}{2} + ab\right) + 2cI\right], \tag{2.51}$$

where

$$I(v) = \frac{1}{\pi}v.p.\int_a^b \frac{\sqrt{(s^2 - a^2)(b^2 - s^2)}\,\mathrm{d}s}{s - v}. \tag{2.52}$$

Now we calculate $U(a)$. As long as $S(a) = 0$ this expression is purely real. After tedious calculations we find that

$$U(\varepsilon) = \frac{8b}{(1-\varepsilon)^2}\left[-\frac{1}{4} - \varepsilon + \frac{1}{2}\varepsilon^2 + \varepsilon^3 + I(\varepsilon)\right], \tag{2.53}$$

here, $\varepsilon = a/b$ and

$$I(\varepsilon) = \frac{1}{\pi}\int_\varepsilon^1 \sqrt{\frac{(q+\varepsilon)(1-q^2)}{q-\varepsilon}}\mathrm{d}q. \tag{2.54}$$

This integral is expressed in terms of elliptic functions, but we will not provide explicit formulas. We study the asymptotic behaviour of $I(\varepsilon)$ at $\varepsilon \to 0$. To do this we use the expansion

$$\sqrt{\frac{q+\varepsilon}{q-\varepsilon}} = 1 + \frac{\varepsilon}{q} + \sum_{k=0}^{\infty} c_k \left(\frac{\varepsilon}{q}\right)^{k+2}. \tag{2.55}$$

Thus we must estimate the integral

$$I(\varepsilon) = \frac{1}{\pi}\int_\varepsilon^1 \left(1 + \frac{\varepsilon}{q} + \sum_{k=0}^{\infty} c_k \left(\frac{\varepsilon}{q}\right)^{k+2}\right)\sqrt{1-q^2}\,\mathrm{d}q. \tag{2.56}$$

Now we mention that

$$\frac{1}{\pi}\int_0^1 \sqrt{1-q^2}\,\mathrm{d}q = \frac{1}{4}. \tag{2.57}$$

One can show that

$$U(\varepsilon) = 8b\left(-\frac{1}{4} + \frac{1}{4} + \frac{1}{\pi}\varepsilon \ln \varepsilon + O(\varepsilon)\right), \tag{2.58}$$

and therefore

$$U(\varepsilon) = \frac{8b}{\pi}\varepsilon \ln \varepsilon + O(\varepsilon), \tag{2.59}$$

where $O(\varepsilon)$ denotes terms of order ε and all higher orders. It is not necessary to determine them precisely.

We end up with the following result:

$$U(a) \to \frac{8}{\pi} a \ln \frac{a}{b} + O(a) \quad \text{at } a \to 0. \tag{2.60}$$

The differential equation

$$\dot{a} = \frac{8}{\pi} a \ln \frac{a}{b} \tag{2.61}$$

with initial data

$$\ln \frac{a}{b} = -\ln \frac{b}{a_0} = -c, \tag{2.62}$$

gives solution

$$\ln \frac{a}{b} = -c \exp\left(\frac{8t}{\pi}\right), \tag{2.63}$$

and

$$a = b \exp\left(-c \exp\left(\frac{8t}{\pi}\right)\right) \quad c = -\ln \frac{b}{a_0}. \tag{2.64a,b}$$

This means that singularity $a = 0$ is never achieved in a finite time, while it approaches the real line faster than exponential estimates predict.

It is important to emphasize that this conclusion will hold only provided that no singularity from the second sheet crosses the branch cut and invalidates the assumption of a single pair of branch points in the first Riemann sheet. Nevertheless, numerical evidence suggests that at least one such solution does exist, see the figure 2(*a*) in Dyachenko *et al.* (2021)

3. Conclusion

A potential fluid flow in the 2-D Euler equations with a free boundary is considered with V and R having a pair of square-root branch points $w = \mathrm{i}a$ and $w = \mathrm{i}b$ in the conformal plane. We obtain the following main results:

(i) The equations of motion have been transplanted to the cut connecting ia to ib in the w-plane, and we introduced a new conformal mapping $\chi(w)$ that allows the study of singularities in higher Riemann sheets. With the second sheet of the w-plane unfolded, one can study the singularities in multiple sheets, and possibly obtain new integrals of motion from pairs of cuts in higher sheets. This conjecture will have implications for a further study of the integrability of water waves.

(ii) We developed an asymptotic theory based on the exact equations formulated at the cut that shows a double-exponential rate of approach of the singularity at $w = \mathrm{i}a(t)$ to the fluid domain. The presented theoretical answers to a long-standing question about the formation of a singularity at the free surface in finite vs infinite time when no gravity or capillarity is present. However, it remains unclear whether a solution with only a single pair of branch points in the first sheet can exist for infinite time.

(iii) The physical fluid can be complemented with a virtual fluid, which is a mathematical object whose motion is defined by the analytic continuation of R and V into $\mathbb{C}^+$ excluding the branch cut. The expanded domain contains a virtual fluid vortex sheet, for which Kelvin's theorem for circulation holds true: a 'virtual circulation' is conserved and is one of the two new invariants discovered in this work. The second invariant, the 'winding', is related to the genus of conformal plane of the virtual fluid – the number of holes.

The present work offers a new look at the problem of water waves and illustrates a deeply rooted connection between water waves and the vortex sheet problem that was overlooked by the water waves community. Despite the fact that the present work is devoted to only a pair of square-root branch points, one may consider a general system of many pairs of branch points connected by branch cuts, $\gamma_k(t)$. The equations for analytic functions R and V are then formed at each $\gamma_k(t)$ and fully determine the flow of the 'virtual fluid'. Each of the branch cuts, $\gamma_k(t)$ is equivalent to a 'virtual' vortex sheet, whose dynamics is governed by the 2-D Euler equations. An open question one could address is related to the rolling of a vortex sheet: Is breaking of a steep water wave related to instabilities of a 'virtual' vortex sheet? The answer to this question is presently a work in progress.

Each pair of square-root branch points is associated with a new pair of integrals of motion: 'winding' and virtual 'circulation'. A particle analogy springs into mind. Nevertheless, these invariants alone do not fully describe the fluid flow, this follows from (2.31), which requires all Fourier modes to be defined, however, 'winding' and 'circulation' only define the first Fourier modes of R and V. Nevertheless, the conformal domain $\chi(w)$ opens the second Riemann sheet for R and V which must contain more singularities and fully define the analytic functions R and V at the cuts. We conjecture that tracking of all singularities and their associated invariants uniquely describes the fluid flow, and these variables are analogous to the 'action' variables in the long standing problem of integrability of 2-D potential Euler equations.

Funding. Studies presented in §§ 2.4 and 2.5 were supported by the Russian Science Foundation grant no. 19-72-30028. The work of V.E.Z. was supported by the National Science Foundation, grant no. DMS-1715323. The work of S.A.D. was supported by the National Science Foundation, grants no. DMS-1716822 and no. DMS-2039071. This material is based upon the work supported by the National Science Foundation under Grant No. DMS-1439786 while S.A.D. was in residence at the Institute for Computational and Experimental Research in Mathematics in Providence, RI, during a part of the Hamiltonian Methods in Dispersive and Wave Evolution Equations program.

Declaration of interests. The authors report no conflict of interest.

Author ORCIDs.
A.I. Dyachenko https://orcid.org/0000-0001-6103-0316;
S.A. Dyachenko https://orcid.org/0000-0003-1265-4055.

Appendix A. Derivation of U and B

We will provide a derivation for the function B, and a calculation for U can be done analogously. Let us consider the product

$$\bar{V}V = \frac{1}{\pi^2}\iint \frac{v(\tau)\bar{v}(\tau')\,\mathrm{d}\tau\,\mathrm{d}\tau'}{(\tau+\mathrm{i}w)(\tau'-\mathrm{i}w)}, \tag{A1}$$

and use the relation

$$\frac{1}{(\tau+\mathrm{i}w)(\tau'-\mathrm{i}w)} = \frac{1}{\tau+\tau'}\left[\frac{1}{\tau+\mathrm{i}w}+\frac{1}{\tau'-\mathrm{i}w}\right]. \tag{A2}$$

The product $\bar{V}V$ then becomes

$$\bar{V}V = \frac{1}{\pi}\int\left[\frac{1}{\pi}\int\frac{\bar{v}(\tau')\,\mathrm{d}\tau'}{\tau'+\tau}\right]\frac{v(\tau)\,\mathrm{d}\tau}{\tau+\mathrm{i}w} + \frac{1}{\pi}\int\left[\frac{1}{\pi}\int\frac{v(\tau)\,\mathrm{d}\tau}{\tau+\tau'}\right]\frac{\bar{v}(\tau)\,\mathrm{d}\tau'}{\tau'-\mathrm{i}w}. \tag{A3}$$

One can observe that the terms enclosed in square bracket are given by the following:

$$V(-\mathrm{i}\tau') = -\frac{1}{\pi}\int\frac{v(\tau)\,\mathrm{d}\tau}{\tau+\tau'} \quad\text{and}\quad \bar{V}(\mathrm{i}\tau) = -\frac{1}{\pi}\int\frac{\bar{v}(\tau')\,\mathrm{d}\tau'}{\tau'+\tau}, \tag{A4a,b}$$

and result in the following formula for $\bar{V}V$:

$$\bar{V}V = -\frac{1}{\pi}\int\frac{v(\tau)\bar{V}(\mathrm{i}\tau)\,\mathrm{d}\tau}{\tau+\mathrm{i}w} - \frac{1}{\pi}\int\frac{\bar{v}(\tau)V(-\mathrm{i}\tau)}{\tau-\mathrm{i}w} = \hat{P}^-\left[\bar{V}V\right]+\hat{P}^+\left[\bar{V}V\right]. \tag{A5}$$

Thus, the function $B(w)$ is defined in the complex plane via

$$B(w) = -\frac{1}{\pi}\int\frac{v(\tau)\bar{V}(\mathrm{i}\tau)\,\mathrm{d}\tau}{\tau+\mathrm{i}w} = -\frac{1}{\pi}\int\frac{b(\tau)\,\mathrm{d}\tau}{\tau+\mathrm{i}w}, \tag{A6}$$

where we defined $b(\tau) := v(\tau)\bar{V}(\mathrm{i}\tau)$ at the interval $\tau\in[a,b]$ to be the jump at the branch cut. Analogous calculation for U results in

$$U(w) = -\frac{1}{\pi}\int\frac{u(\tau)\,\mathrm{d}\tau}{\tau+\mathrm{i}w} = -\frac{1}{\pi}\int\frac{\left[v(\tau)\bar{R}(\mathrm{i}\tau)+r(\tau)\bar{V}(\mathrm{i}\tau)\right]\mathrm{d}\tau}{\tau+\mathrm{i}w}, \tag{A7}$$

where we defined $u(\tau) := v(\tau)\bar{R}(\mathrm{i}\tau)+r(\tau)\bar{V}(\mathrm{i}\tau)$ at the interval $\tau\in[a,b]$.

Appendix B. Supplemental relations with Chebyshev polynomials

We consider an auxiliary contour integral around interval $[-1,1]$ and apply residue theorem

$$I = \oint_{[-1,1]}\frac{(T_n(x)+\sqrt{x^2-1}U_{n-1}(x))\mathrm{d}x}{x+y} = \oint_{[-1,1]}\frac{(x+\sqrt{x^2-1})^n\mathrm{d}x}{x+y}, \tag{B1}$$

where we used the following identity for Chebyshev polynomials:

$$T_n(x)+\sqrt{x^2-1}U_{n-1}(x) = (x+\sqrt{x^2-1})^n. \tag{B2}$$

We consider the branch of square root $\sqrt{x^2-1} = \mathrm{i}\sqrt{1-x^2}$ above the cut, and $\sqrt{x^2-1} = -\mathrm{i}\sqrt{1-x^2}$ below. The auxiliary integral I is related to integral of interest by the following

formula:

$$\int_{-1}^{1}\frac{\sqrt{1-x^2}U_{n-1}(x)\,\mathrm{d}x}{x+y}=\frac{1}{2\mathrm{i}}\oint_{[-1,1]}\frac{(T_n(x)+\sqrt{x^2-1}U_{n-1}(x))\mathrm{d}x}{\xi+y}=\frac{I}{2\mathrm{i}},\tag{B3}$$

where we have noted that integral of regular function $T_n(x)/(x+y)$ around a closed curve vanishes. The contour integral I consists of four parts, however, circular integrals around $x=\pm1$ vanish because the integrand has no poles at these points, therefore leaving only the two integrals above and below the cut

$$I=\int_{-1}^{1}\frac{(x+\mathrm{i}\sqrt{1-x^2})^n-(x-\mathrm{i}\sqrt{1-x^2})^n}{x+y}\mathrm{d}x.\tag{B4}$$

We make a substitution $x=\cos t$, $0<t<\pi$ and symmetrize the interval of integration

$$I=\int_{\pi}^{0}\frac{\exp(int)-\exp(-int)}{\cos(t)+y}(-\sin t)\,\mathrm{d}t=\frac{1}{2}\int_{-\pi}^{\pi}\frac{\exp(int)-\exp(-int)}{\cos t+y}\sin t\,\mathrm{d}t,\tag{B5}$$

and after the substitution $z=\mathrm{e}^{\mathrm{i}t}$, $|z|=1$ and $\mathrm{d}t=\mathrm{d}z/\mathrm{i}z$

$$I=-\frac{1}{2}\oint_{|z|=1}\frac{\left(z^n-z^{-n}\right)\left(z-z^{-1}\right)}{z^2+2yz+1}\mathrm{d}z.\tag{B6}$$

The integrand has a pole of order $(n+3)$ at $z=0$ and a pair of simple poles at $z=-y\pm\sqrt{y^2-1}$. When $y=\xi+2+2a/l>1$, only the poles at $z=0$ and $z=-y+\sqrt{y^2-1}$ lie within the unit circle. Note that poles switch if $y<-1$! Also it is straightforward to obtain result for complex y.

The residues at $z=-y\pm\sqrt{y^2-1}$ can be computed explicitly and by virtue of (B2) are given by

$$\operatorname*{Res}_{-y\pm\sqrt{y^2-1}}\frac{(z^n-z^{-n})(z-z^{-1})}{z^2+2yz+1}=\pm2\sqrt{y^2-1}U_{n-1}(-y),\tag{B7}$$

where we used symmetry for Chebyshev polynomials of even and odd n.

For the residue at zero we first note the generating function of Chebyshev polynomials

$$\frac{(z^n-z^{-n})(z-z^{-1})}{1+2yz+z^2}=\left(z^n-\frac{1}{z^n}\right)\left(z-\frac{1}{z}\right)\sum_{k=0}^{\infty}U_k(-y)z^k,\tag{B8}$$

to write Laurent series, and note that only the following terms contribute to the principal part:

$$\frac{1}{z^{n+1}}\sum_{k=0}^{\infty}U_k(-y)z^k-\frac{1}{z^{n-1}}\sum_{k=0}^{\infty}U_k(-y)z^k,\tag{B9}$$

and the residues are

$$\left.\begin{array}{ll}U_1(-y), & n=1\\ U_n(-y)-U_{n-2}(-y), & n>1.\end{array}\right\}\tag{B10}$$

It is convenient to use recursion relations for Chebyshev polynomials $2T_n(x)=U_n(x)-U_{n-2}(x)$ and $2T_1(x)=U_1(x)$ to have the residue written in the compact form

$$\operatorname*{Res}_{z=0}\frac{(z^n-z^{-n})(z-z^{-1})}{z^2+2yz+1}=2T_n(-y).\tag{B11}$$

The final result for $y > 1$ is obtained by summing the two residues (B7) and (B11)

$$\frac{1}{\pi}\int_{-1}^{1}\frac{\sqrt{1-x^2}U_{n-1}(x)\,\mathrm{d}x}{x+y} = -\left[T_n(-y)+\sqrt{y^2-1}U_{n-1}(-y)\right] = -\left(\sqrt{y^2-1}-y\right)^n. \tag{B12}$$

Note that this can be extended for $-1 < y < 1$, as follows:

$$\frac{1}{\pi}p.v.\int_{-1}^{1}\frac{\sqrt{1-x^2}U_{n-1}(x)\,\mathrm{d}x}{x-y} = -T_n(y). \tag{B13}$$

References

Ablowitz, M.J., Kaup, D.J., Newell, A.C. & Segur, H. 1974 The inverse scattering transform-fourier analysis for nonlinear problems. *Stud. Appl. Maths* **53** (4), 249–315.

Alpert, B., Greengard, L. & Hagström, T. 2000 Rapid evaluation of nonreflecting boundary kernels for time-domain wave propagation. *SIAM J. Numer. Anal.* **37** (4), 1138–1164.

Ambrose, D.M., Camassa, R., Marzuola, J.L., McLaughlin, R.M., Robinson, Q. & Wilkening, J. 2022 Numerical algorithms for water waves with background flow over obstacles and topography. *Adv. Comput. Math.* **48** (4), 1–62.

Arsénio, D., Dormy, E. & Lacave, C. 2020 The vortex method for two-dimensional ideal flows in exterior domains. *SIAM J. Math. Anal.* **52** (4), 3881–3961.

Baker, G.R. & Xie, C. 2011 Singularities in the complex physical plane for deep water waves. *J. Fluid Mech.* **685**, 83–116.

Castro, A., Córboda, D., Fefferman, C., Gancedo, F. & Gómez-Serrano, J. 2013 Finite time singularities for the free boundary incompressible euler equations. *Ann. Math.* **178** (3), 1061–1134.

Crapper, G.D. 1957 An exact solution for progressive capillary waves of arbitrary amplitude. *J. Fluid Mech.* **2**, 532–540.

Crowdy, D.G. 2000 A new approach to free surface euler flows with capillarity. *Stud. Appl. Maths* **105** (1), 35–58.

Dyachenko, A.I. 2001 On the dynamics of an ideal fluid with a free surface. *Dokl. Math.* **63**, 115–117.

Dyachenko, A.I., Dyachenko, S.A., Lushnikov, P.M. & Zakharov, V.E. 2019 Dynamics of poles in two-dimensional hydrodynamics with free surface: new constants of motion. *J. Fluid Mech.* **874**, 891–925.

Dyachenko, A.I., Dyachenko, S.A., Lushnikov, P.M. & Zakharov, V.E. 2021 Short branch cut approximation in two-dimensional hydrodynamics with free surface. *Proc. R. Soc.* A **477** (2249), 20200811.

Dyachenko, A.I., Kuznetsov, E.A., Spector, M.D. & Zakharov, V.E. 1996 Analytical description of the free surface dynamics of an ideal fluid (canonical formalism and conformal mapping). *Phys. Lett.* A **221** (1), 73–79.

Dyachenko, A.I., Lvov, Y.V. & Zakharov, V.E. 1995 Five-wave interaction on the surface of deep fluid. *Physica* D **87** (1–4), 233–261.

Dyachenko, A.I., Zakharov, V.E. & Kuznetsov, E.A. 1996 Nonlinear dynamics of the free surface of an ideal fluid. *Plasma Phys. Rep.* **22** (10), 829–840.

Dyachenko, S.A., Lushnikov, P.M. & Korotkevich, A.O. 2014 Complex singularity of a stokes wave. *JETP Lett.* **98** (11), 675–679.

Dyachenko, S.A., Lushnikov, P.M. & Korotkevich, A.O. 2016 Branch cuts of stokes wave on deep water. Part 1. Numerical solution and Padé approximation. *Stud. Appl. Maths* **137** (4), 419–472.

Dyachenko, S.A. & Mikyoung Hur, V. 2019 Stokes waves with constant vorticity: folds, gaps and fluid bubbles. *J. Fluid Mech.* **878**, 502–521.

Dyachenko, S.A. & Newell, A.C. 2016 Whitecapping. *Stud. Appl. Maths* **137** (2), 199–213.

Galin, L.A. 1945 Unsteady filtration with a free surface. *C. R. L'Acad. Sci. l'URSS* **47**, 246–249.

Gardner, C.S., Greene, J.M., Kruskal, M.D. & Miura, R.M. 1967 Method for solving the Korteweg-Devries equation. *Phys. Rev. Lett.* **19** (19), 1095.

Grant, M.A. 1973 The singularity at the crest of a finite amplitude progressive Stokes wave. *J. Fluid Mech.* **59** (2), 257–262.

Haziot, S.V., Mikyoung Hur, V., Strauss, W., Toland, J.F., Wahlén, E., Walsh, S. & Wheeler, M.H. 2022 Traveling water waves – the ebb and flow of two centuries. *Quart. Appl. Math.* **80** (2), 317–401.

Karabut, E.A. & Zhuravleva, E.N. 2014 Unsteady flows with a zero acceleration on the free boundary. *J. Fluid Mech.* **754**, 308–331.

KARABUT, E.A., ZHURAVLEVA, E.N. & ZUBAREV, N.M. 2020 Application of transport equations for constructing exact solutions for the problem of motion of a fluid with a free boundary. *J. Fluid Mech.* **890**, A13.

KOLMOGOROV, A.N. 1954 On the conservation of conditionally periodic motions under small perturbation of the Hamiltonian. In *Dokl. Akad. Nauk SSSR* **98** (527), 2–3.

KUZNETSOV, E.A., SPECTOR, M.D. & ZAKHAROV, V.E. 1993 Surface singularities of ideal fluid. *Phys. Lett.* A **182** (4–6), 387–393.

LIU, J.-G. & PEGO, R.L. 2021 In search of local singularities in ideal potential flows with free surface. arXiv:2108.00445.

LONGUET-HIGGINS, M.S. 1972 A class of exact, time-dependent, free-surface flows. *J. Fluid Mech.* **55** (3), 529–543.

LUSHNIKOV, P.M. 2016 Structure and location of branch point singularities for stokes waves on deep water. *J. Fluid Mech.* **800**, 557–594.

LUSHNIKOV, P.M. & ZAKHAROV, V.E. 2021 Poles and branch cuts in free surface hydrodynamics. *Water Waves* **3**, 251–266.

MIKYOUNG HUR, V. & WHEELER, M.H. 2020 Exact free surfaces in constant vorticity flows. *J. Fluid Mech.* **896**, R1.

OVSYANNIKOV, L.V. 1973 Dynamika sploshnoi sredy, lavrentiev institute of hydrodynamics. *Sib. Branch Acad. Sci. USSR* **15**, 104.

POLUBARINOVA-KOCHINA, P.Y. 1945 On the displacement of the oil-bearing contour. *C. R. L'Acad. Sci. l'URSS* **47**, 250–254.

SHABAT, A. & ZAKHAROV, V. 1972 Exact theory of two-dimensional self-focusing and one-dimensional self-modulation of waves in nonlinear media. *Sov. Phys. JETP* **34** (1), 62.

STOKES, G.G. 1880 *Mathematical and Physical Papers*, vol. 1. Cambridge University Press.

TANVEER, S. 1991 Singularities in water waves and Rayleigh–Taylor instability. *Proc. R. Soc. Lond.* A **435** (1893), 137–158.

TANVEER, S. 1993 Singularities in the classical Rayleigh–Taylor flow: formation and subsequent motion. *Proc. R. Soc. Lond.* A **441** (1913), 501–525.

WILKENING, J. 2021 Traveling-standing water waves. *Fluids* **6** (5), 187.

WILKENING, J. & VASAN, V. 2015 Comparison of five methods of computing the dirichlet-neumann operator for the water wave problem. *Contemp. Maths* **635**, 175–210.

ZAKHAROV, V.E. 1968 Stability of periodic waves of finite amplitude on the surface of a deep fluid. *J. Appl. Mech. Tech. Phys.* **9** (2), 190–194.

ZAKHAROV, V.E. 2020 Integration of a deep fluid equation with a free surface. *Theor. Math. Phys.* **202** (3), 285–294.

ZAKHAROV, V.E. & DYACHENKO, A.I. 1996 High-jacobian approximation in the free surface dynamics of an ideal fluid. *Physica* D **98** (2), 652–664.

ZAKHAROV, V.E., DYACHENKO, A.I. & VASILYEV, O.A. 2002 New method for numerical simulation of a nonstationary potential flow of incompressible fluid with a free surface. *Eur. J. Mech.* B*/Fluids* **21** (3), 283–291.

ZAKHAROV, V.E. & FADDEEV, L.D. 1971 Korteweg–de vries equation: a completely integrable hamiltonian system. *Funktsional'nyi Analiz i ego Prilozheniya* **5** (4), 18–27.

ZAKHAROV, V.E. & SHABAT, A.B. 1974 A scheme for integrating the nonlinear equations of mathematical physics by the method of the inverse scattering problem. I. *Funktsional'nyi Analiz i ego Prilozheniya* **8** (3), 43–53.

ZAKHAROV, V.E. & SHABAT, A.B. 1979 Integration of nonlinear equations of mathematical physics by the method of inverse scattering. II. *Funct. Anal. Applics.* **13** (3), 166–174.